

Consideration of the cross sectional profile of the Booster vacuum chamber

G. F. Dell

April 1987

Collider Accelerator Department
Brookhaven National Laboratory

U.S. Department of Energy

USDOE Office of Science (SC)

Notice: This technical note has been authored by employees of Brookhaven Science Associates, LLC under Contract No.DE-AC02-76CH00016 with the U.S. Department of Energy. The publisher by accepting the technical note for publication acknowledges that the United States Government retains a non-exclusive, paid-up, irrevocable, world-wide license to publish or reproduce the published form of this technical note, or allow others to do so, for United States Government purposes.

DISCLAIMER

This report was prepared as an account of work sponsored by an agency of the United States Government. Neither the United States Government nor any agency thereof, nor any of their employees, nor any of their contractors, subcontractors, or their employees, makes any warranty, express or implied, or assumes any legal liability or responsibility for the accuracy, completeness, or any third party's use or the results of such use of any information, apparatus, product, or process disclosed, or represents that its use would not infringe privately owned rights. Reference herein to any specific commercial product, process, or service by trade name, trademark, manufacturer, or otherwise, does not necessarily constitute or imply its endorsement, recommendation, or favoring by the United States Government or any agency thereof or its contractors or subcontractors. The views and opinions of authors expressed herein do not necessarily state or reflect those of the United States Government or any agency thereof.

CONSIDERATION OF THE CROSS SECTIONAL PROFILE
OF THE BOOSTER VACUUM CHAMBER

AD

Booster Technical Note
No. 76

G. F. DELL

APRIL 8, 1987

ACCELERATOR DEVELOPMENT DEPARTMENT
Brookhaven National Laboratory
Upton, N.Y. 11973

Consideration of the Cross Sectional Profile of the Booster Vacuum Chamber

G.F. Dell

During injection the closed orbit is displaced in superperiod "C" by a combination of a slow and fast beam bump. Initially the closed orbit is displaced to the center of the injection channel and injection may continue for as long as 300 μ sec as the orbit bump is decreased. The position of the injection channel relative to the centerline of the vacuum chamber (and therefore the size of the orbit bump) is still flexible, however in the present study a worst case scenario is considered for which injection occurs at the maximum distance from the chamber centerline (~ 75 mm). This scenario is considered to determine whether or not injection imposes special constraints on the cross sectional profile of the vacuum chamber.

1). A vacuum chamber having an outside dimension of ~ 6 inches and a wall thickness of 0.075" is assumed (This is sample #2 considered in Booster Tech Note #63)¹. The inner half width is 75 mm (See Figure 1). For this chamber the height is 2.746" at the center and 2.246" at the edge. The sag at the center is 0.180" after evacuation and is assumed zero at the edge; the chamber walls are 0.075" thick. This gives a vertical half aperture $A_y(x) = 26.62 + 4.06((75-x(\text{mm}))/75)$, and thus at $x=0$, $A_y(0)=30.68$ mm, and at $x=40$ mm, $A_y(40)=28.5$ mm.

2). The proton beam from the linac is said to have equal horizontal and vertical emittances of $\epsilon_x = \epsilon_y = 5\pi$ mm mrad². At the point of injection (near quadrupole CQ5), $\beta_x = 13.55$ m and $\beta_y = 3.70$ m; this gives intrinsic betatron amplitudes of $X_\beta = 8.2$ mm and $Y_\beta = 4.3$ mm when the beam is injected on the booster closed orbit. Consequently the maximum allowed beam bump consistent with the injected beam just missing the chamber wall is $75 - 8.2 = 67$ mm.

3). The beam bump profile of Y.Y. Lee³ for a maximum closed orbit displacement of 50 mm (See Figure 2) has been scaled to 67 mm. The displacements at various elements, as well as the beta functions at these elements, are listed in Table 1.

4). The definition of geometry used in this study is shown in Figure 3. X_{c0} denotes the distance of the closed orbit from the chamber centerline, and ΔX denotes the distance of the closed orbit from the center of the injection channel. At all times $X_{c0} + \Delta X = 67$ mm. At the start of injection the closed orbit is at the center of the injection channel ($\Delta X = 0$). As injection progresses, the orbit bump decreases; ΔX increases and is an additional betatron amplitude relative to the closed orbit: $X_{\beta} = X_{\beta_0} + \Delta X$.

5). Tracking studies have shown the presence of coupling with essentially total emittance transfer back and forth between the horizontal and vertical planes. Regardless of the presence or absence of coupling, the vertical acceptance is limited by the lattice optics. The vertical beta function is largest at the defocusing quadrupoles; the relation between vertical amplitudes $Y(QF)$ and $Y(QD)$ at the QF and QD quadrupoles is: $Y(QF) = (\beta_y(QF) / \beta_y(QD))^{1/2} Y(QD) = 0.52 Y(QD)$ -- the beam height at the focusing quadrupoles is limited by the aperture of the defocusing quadrupoles.

The main effect of coupling is to limit the range of ΔX over which the beam can be injected. Large coupling causes the vertical beam size to increase, while zero coupling would cause no increase in beam height and would enable a flat, ribbon beam to be injected.

- 6). Figure 4 shows several possible stages of injection.
- a). Start of injection. The closed orbit is at the center of the injection channel ($\Delta X=0$). The beam is indicated by the hatched area.
 - b). Injection when the closed orbit has moved ~ 25 mm from the center of the injection channel ($\Delta X=25$ mm). The case of zero coupling is shown; the shaded area indicates a ribbon beam with half height of 4.3 mm.
 - c). Same condition as case b), but with emittance transfer such that $\epsilon_x = \epsilon_y$. The horizontal dimension of the beam has decreased while the half height of the beam has increased to 12.9 mm. This configuration corresponds to $\epsilon_x' / \pi = (25+8.2)^2 / 13.55 = 81$ mm mrad.

7). The horizontal and vertical extremes of a test particle have been determined at several key elements around the injection region as the beam bump is decreased ($\Delta X = 0, 8, 16, 24,$ and 32 mm) and for several values of emittance transfer k from the horizontal to the vertical plane. With $\epsilon_x' = (\Delta X + X_{\beta_0})^2 / \beta_x$, horizontal and vertical limits have been determined when $k = 0, 0.2, 0.5, 0.7, 0.85,$ and 1.0 when $\epsilon_x = (1-k) \epsilon_x'$ and $\epsilon_y = \epsilon_{y_0} + k \epsilon_x'$. ($\epsilon_{y_0} = 5\pi$ mm mrad).

8). The horizontal and vertical requirements at quadrupole CQ5 are shown in Figure 5(a) for values of ΔX , the corresponding ϵ_x' , and k , the coefficient of emittance transfer listed in Item 7. Dashed lines indicate the dependence on ΔX at fixed coupling, while the solid lines indicate the dependence on coupling at fixed ΔX . The horizontal line at $y=15.5$ mm denotes the maximum allowed vertical amplitude at CQ5 (and other focusing quadrupoles). This maximum is much smaller than the vertical half aperture of the sample #2 chamber of Figure 1 and will be discussed in Item 11. As mentioned above, coupling limits the range of ΔX over which injection can take place, but it does not change the maximum allowed beam height.

9). The horizontal and vertical requirements at the upstream and downstream ends of dipole CD5 are shown in Figures 5(b) and 5(c), respectively. The plots reflect the difference in the displacement of the closed orbit as well as the difference of the horizontal and vertical beta functions at the magnet ends. As before, injection for $\Delta X=16$ mm is acceptable for all emittance transfers, k . Even in the extreme case being considered ($\hat{x}_{CO}=67$ mm), large vertical apertures are not needed for $x>40$ mm.

10). The horizontal and vertical requirements at quadrupoles CQ4 and CQ6 are shown in Figures 5(d) and 5(e), respectively. At these elements the beam bump is no more than half its maximum value at CQ5. As before, injection at $\Delta X=16$ mm is possible at all emittance transfers, k ; injection for larger ΔX is contingent on coupling being less than 100%. In all cases, large aperture is only needed for $x<40$ mm.

11). The section of the Booster where the orbit bump is greatest (CD4 to CD7) is shown in Figure 6. The small "T's" appearing at the center of the vacuum chambers near the ends of the dipoles indicate transitions from the elliptical chambers present in the dipoles to the circular chambers present in the quadrupoles. In this region where the beam bump is largest, only CD5 and CD7 have elliptical chambers. Hence the vertical aperture limitation does not occur at the defocusing quadrupoles but rather at the transition sections nearest the defocusing quadrupoles -- in this case, near the upstream end of dipole CD7. The present Booster lattice has a 30 cm spacing between dipole CD7 and quadrupole CQ6. The transition point is assumed to be at the center of this 30 cm section. At this location, $\beta_y=12.59$ m. Thus $Y(QF)=0.54 Y(T'')$, and the maximum allowed vertical amplitude in CQ5 that is consistent with a horizontal displacement of 40 mm in CQ6 is 15.5 mm.

12). Conclusion. Due to lattice optics, the vertical acceptance of the elliptical vacuum chamber is limited where β_y has its maximum value; this occurs at the transition from elliptical to circular chambers near the defocusing quadrupoles. In all cases the maximum vertical betatron amplitude occurs where the horizontal betatron amplitude is smallest (and vice versa). Thus, except where the beam is purposely displaced off the chamber centerline, large vertical apertures are only needed near the center of the chamber. When the closed orbit is displaced a maximum of 67 mm at CQ5, the region where the orbit bump exceeds 30 mm lies between CQ4 and CD8; in this region where one can have large vertical amplitudes at large displacements, the transition downstream of quadrupole CQ6 represents the worst case. However, both the beam bump and β_y at CQ6 are larger than those at the transition, so the results of Figure 5(e) represent a situation slightly worse than that at the point of transition.

The dashed horizontal lines on Figures 5(a)-(e) indicate the maximum allowed vertical amplitude at each element that is consistent with the conditions at CQ6 (large closed orbit displacement (40 mm) and large vertical beta function, $\beta_y=13.64$ m). In all cases the relation $y(QF) \leq 0.54 \hat{y}(QD)$ cannot be exceeded. The curves of Figures 5(a)-(e) indicate that the present chamber accommodates beam with all degrees of coupling when ΔX is no more than 16 mm. This corresponds to a total emittance $\epsilon_t = \epsilon_x + \epsilon_y \sim 50\pi$ mm mrad and is thought to meet the Booster design parameters; this is discussed below.

With $\epsilon_t = \epsilon_x + \epsilon_y$, consider the ellipse:

$$\frac{\epsilon_x}{\epsilon_t} + \frac{\epsilon_y}{\epsilon_t} = \frac{X^2/\beta_x}{\hat{X}^2/\beta_x} + \frac{Y^2/\epsilon_y}{\hat{Y}^2/\beta_y} = 1.$$

This ellipse satisfies the requirement that $\hat{\epsilon}_x = \epsilon_t$ and $\hat{\epsilon}_y = \epsilon_t$, and when $\epsilon_t = 50\pi$ mm mrad ($\Delta X \sim 16$ mm), the beam easily fits into the vacuum chamber for all degrees of coupling. However, we have normally done particle tracking using the conditions that $\epsilon_x = \epsilon_y$ for $0 \leq \epsilon_x \leq 50\pi$ mm mrad. This second beam corresponds to $\Delta X \sim 27.6$ mm and does not fit into the vacuum chamber when the emittance transfer coefficient k is larger than ~ 0.7 . It is asserted that this second beam having $\epsilon_t = 100\pi$ mm mrad is not that specified for the Booster and that the desired beam having $\epsilon_t \leq 50\pi$ mm mrad fits comfortably into the chambers discussed in Reference (1).

The following conclusions are reached: 1). with zero coupling, there is no vertical restriction, and flat beams can be injected over a large range of ΔX as the beam bump collapses, and 2). with 100% coupling, beams having a total emittance $\epsilon_t = \epsilon_x + \epsilon_y = 50\pi$ mm mrad fit into the vacuum chamber even when the closed orbit is displaced to 67 mm from the chamber centerline. For 100% coupling, injection is limited to an excursion of ΔX satisfying $0 \leq \Delta X \leq 20.4$ mm ($\hat{\epsilon}_t = 65\pi$ mm mrad). For this case the injection channel can be nearer to the chamber centerline and relaxes even farther the requirements on chamber profile at large distances from its centerline.

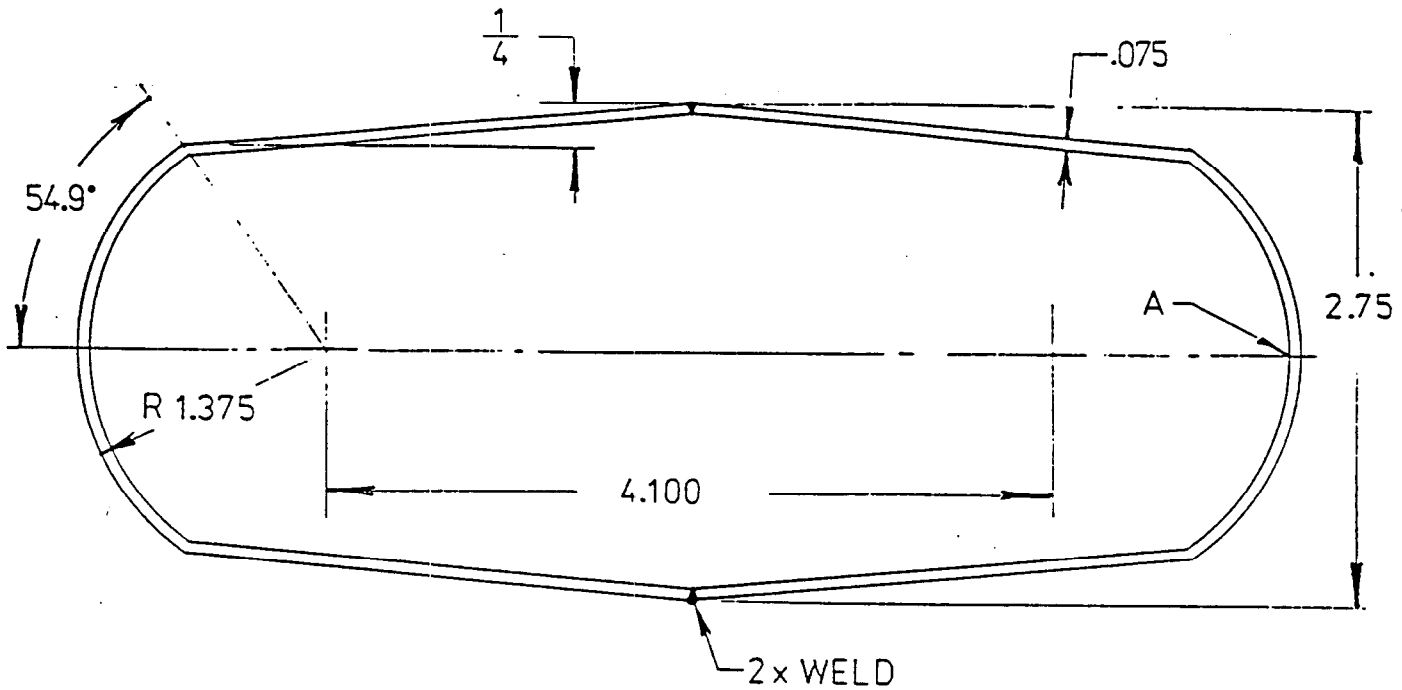
REFERENCES

- 1). B. McDowell, Booster Technical Note No. 63, October 22, 1986.
- 2). Y.Y. Lee. Private communication.
- 3). *ibid.*

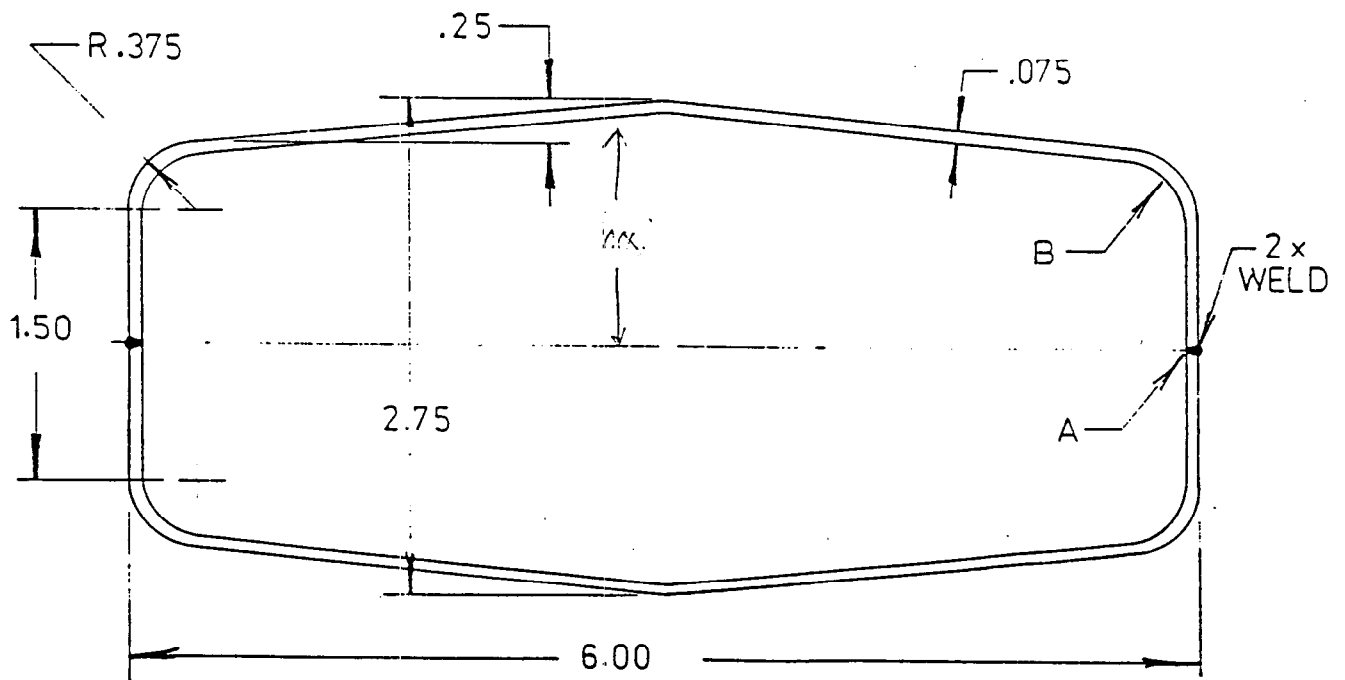
ELEMENT	$\beta_x(m)$	$\beta_y(m)$	$\chi_p(m)$	$\chi_c(mm)$
CQ3	13.33 13.86 13.43	3.85 3.70 3.85	2.778 2.831 2.784	6.4
CD4	12.39 5.82	4.25 9.69	2.669 1.919	16.1
CQ4	4.14 3.98 4.13	13.16 13.64 13.16	1.680 1.650 1.680	25.1
CD5	4.55 9.89	12.04 5.41	1.754 2.515	30.6 43.1 54.6
CQ5	13.11 13.55 13.04	3.85 3.70 3.85	2.905 2.951 2.891	67
CQ6	3.77 3.62 3.78	13.16 13.64 13.16	1.285 1.198 1.156	33.6
CD7	4.20 9.64	12.04 5.41	1.130 1.118	35.2
CQ7	13.00 13.48 13.02	3.85 3.70 3.85	1.193 1.191 1.147	36.8
CD8	11.96 5.41	4.25 9.69	1.070 0.618	21.0
CQ8	3.90 3.64 3.79	13.16 13.64 13.16	0.554 0.510 0.516	-2.20
DD1	4.18 9.45	12.04 5.41	0.565 0.918	-0.03
DQ1	12.70 13.16 12.70	3.85 3.70 3.85	1.148 1.185 1.180	-0.04
T(CD4)	4.35	12.59	1.716	23.6
T(CQ4)	4.34	12.59	1.717	29.2
T(CD5)	10.34	5.13	2.573	56.3
T(CQ6)	3.98	12.59	1.143	34.0

Table 1. Machine functions and orbit bump at various elements in period "C" of the booster. Multiple entries correspond to entrance, center, and exit of the indicated element. "T" indicates a transition from an elliptical to a circular vacuum chamber; T(CD4) denotes the transition at the downstream end of dipole CD4, etc.

7.



Sample 1.
AGS TYPE CHAMBER



Sample 2.

Figure 1. Chamber profiles considered in Booster TN-63. Profiles of both chambers are similar in their decrease of vertical height with increasing distance from the chamber centerline. Sample #2 is considered in the present study.

PROTON INJECTION BUMPS

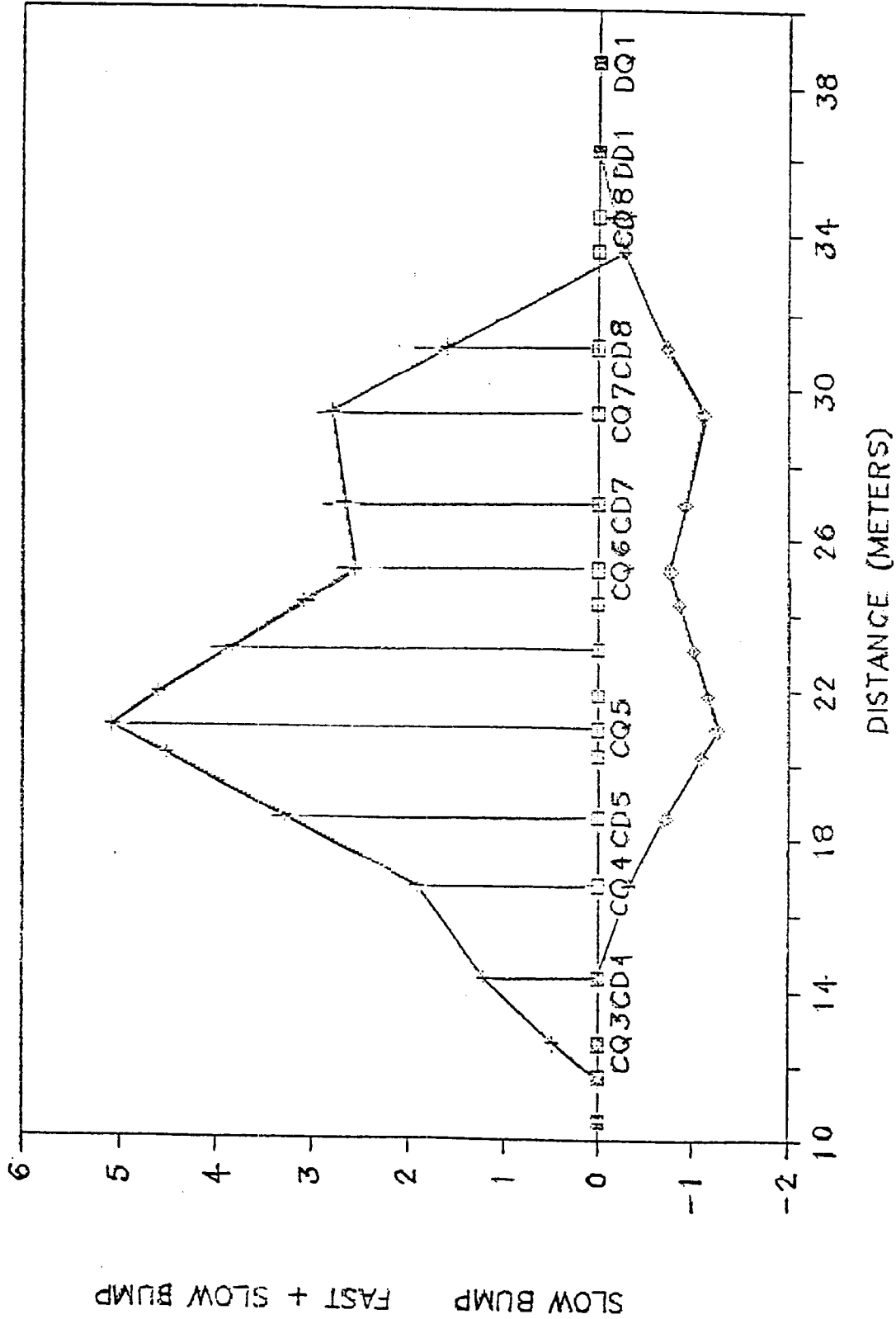
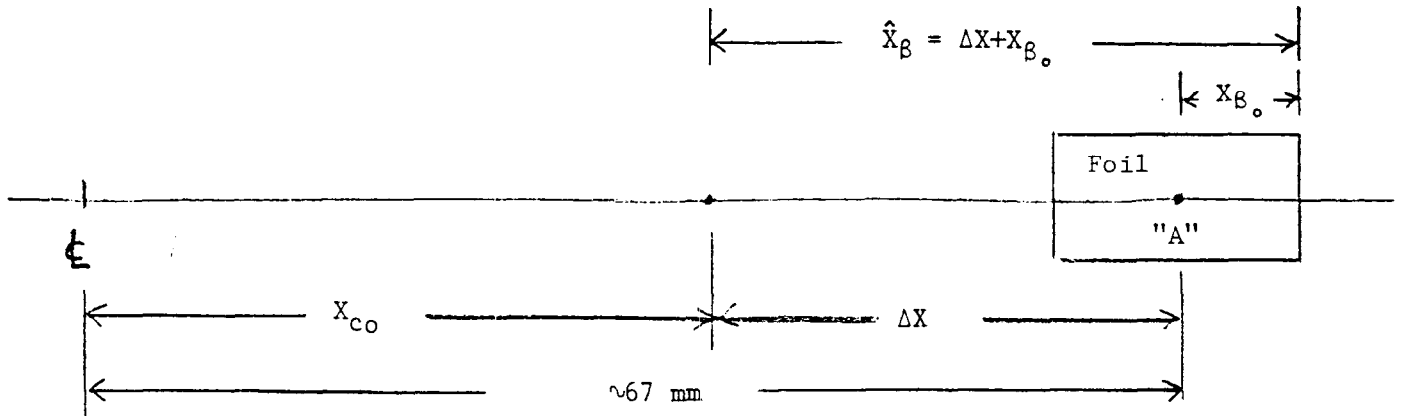
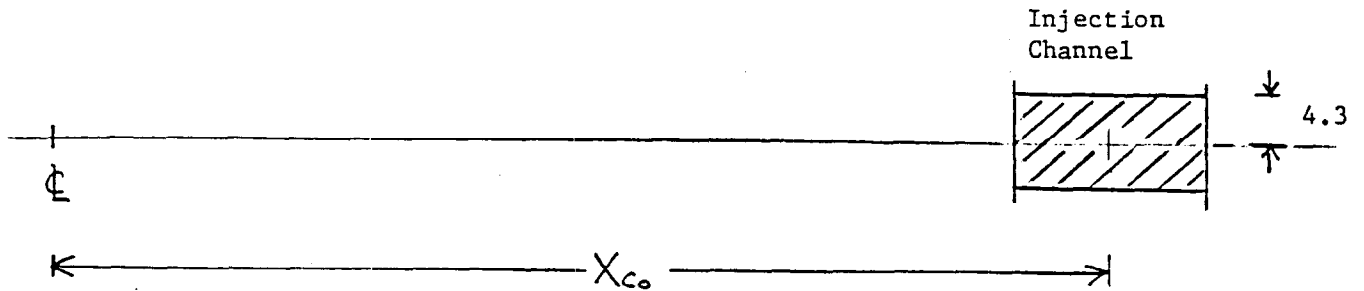


Figure 2. Beam bump profile of Y.Y. Lee. Fast bump has been scaled from a 50 to a 67 mm amplitude to study a worst case scenario.

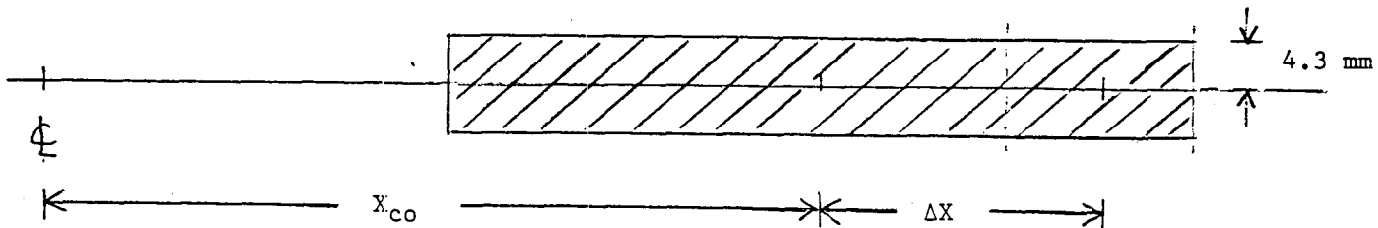


- X_{co} = displacement of the closed orbit from the chamber centerline ϵ .
 ΔX = distance of the closed orbit from "A" (center of the injection channel).
 X_{β_0} = horizontal betatron amplitude of the linac beam.
 \hat{X}_{β} = maximum betatron amplitude of the injected beam relative to the
 closed orbit: $\Delta X - X_{\beta_0} \leq X_{\beta} \leq \Delta X + X_{\beta_0} = \hat{X}_{\beta}$

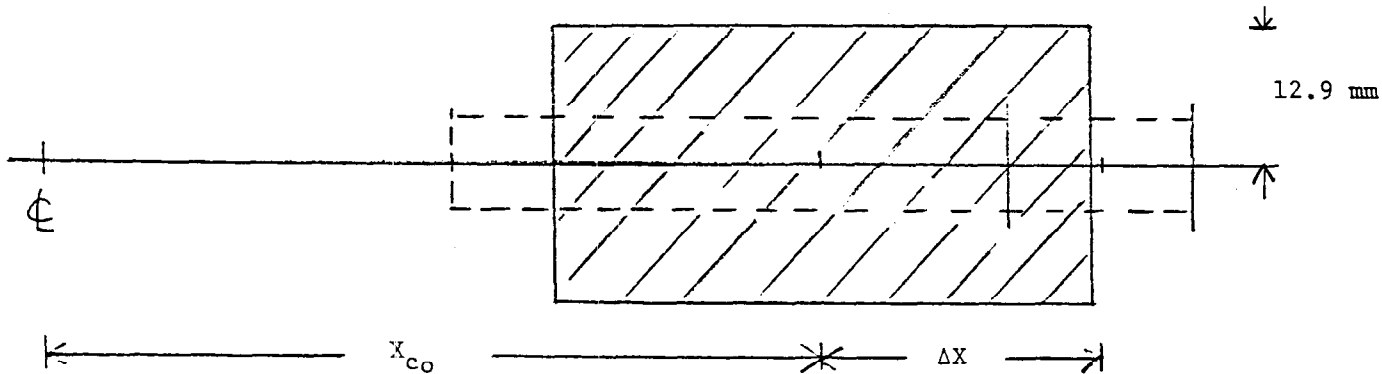
Figure 3. Definition of geometry and symbols used in the present study.



- a). Start of injection; closed orbit is displaced to the center of the injection channel.



- b). Closed orbit bump has decreased by ~ 25 mm producing a flat beam with $\epsilon_x = 85\pi$ mm mrad and $\epsilon_y = 5\pi$ mm mrad. (no coupling).



- c). Closed orbit bump has decreased by ~ 25 mm. Beam cross section corresponds to coupling with $\epsilon_x = \epsilon_y = 45\pi$ mm mrad.

Figure 4. Various cases of injection: a). start of injection when the closed orbit is at the center of the injection channel, b). ribbon beam formed (no coupling) as the beam bump amplitude has decreased by $\Delta X = 25$ mm, and c). beam having $\epsilon_x = \epsilon_y$ when the beam bump has decreased by $\Delta X = 25$ mm. This beam, with $k=0.5$, fits into the vacuum chamber. In the event of total emittance transfer ($k=1.0$), the beam would hit the chamber near the ends of the dipoles nearest defocusing quadrupoles.

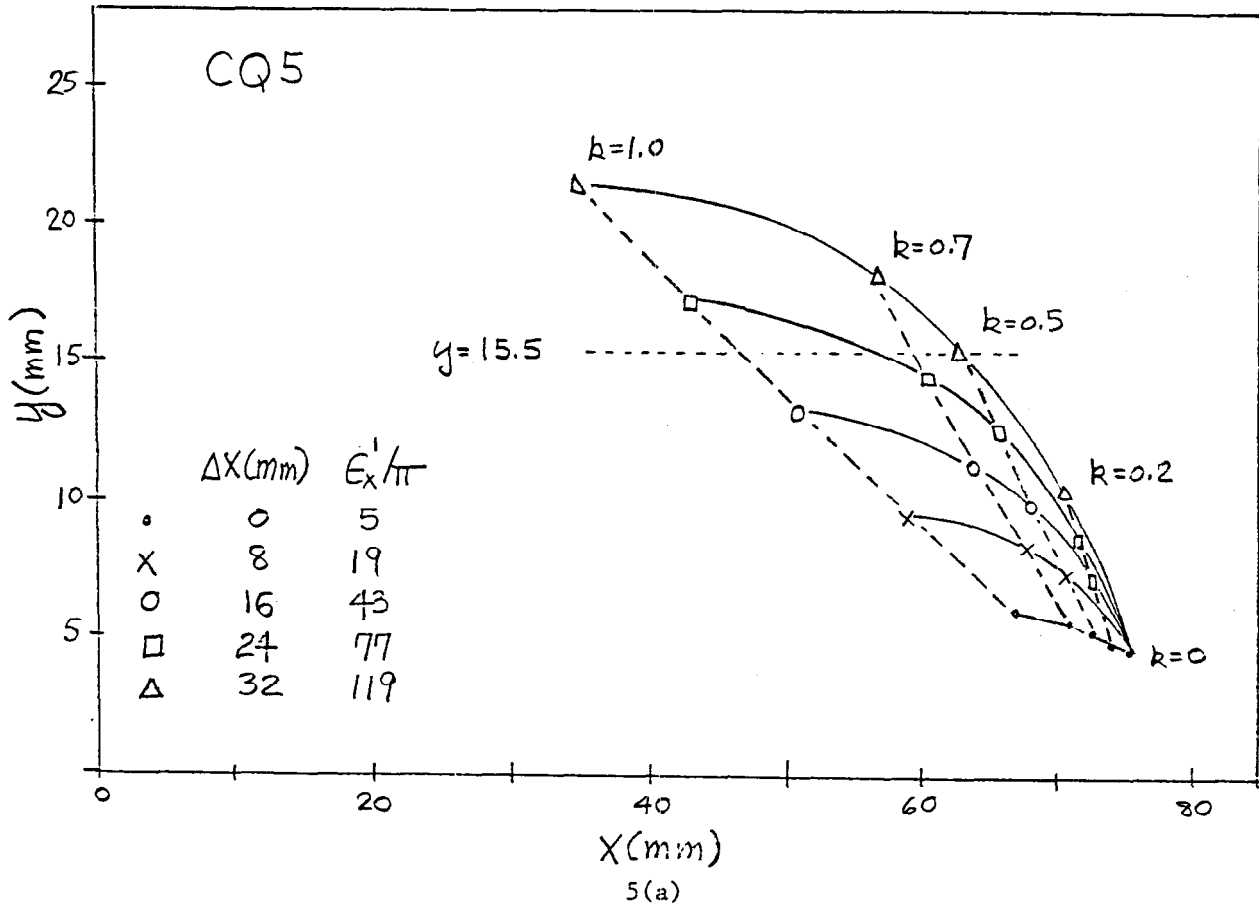
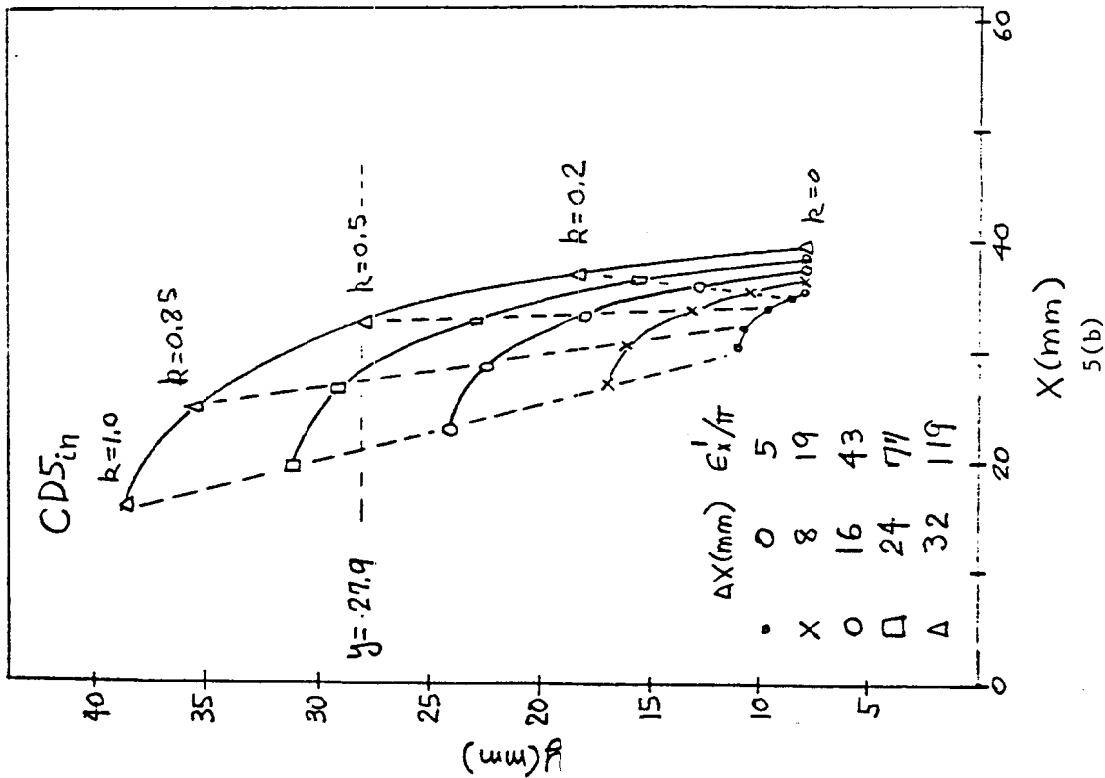
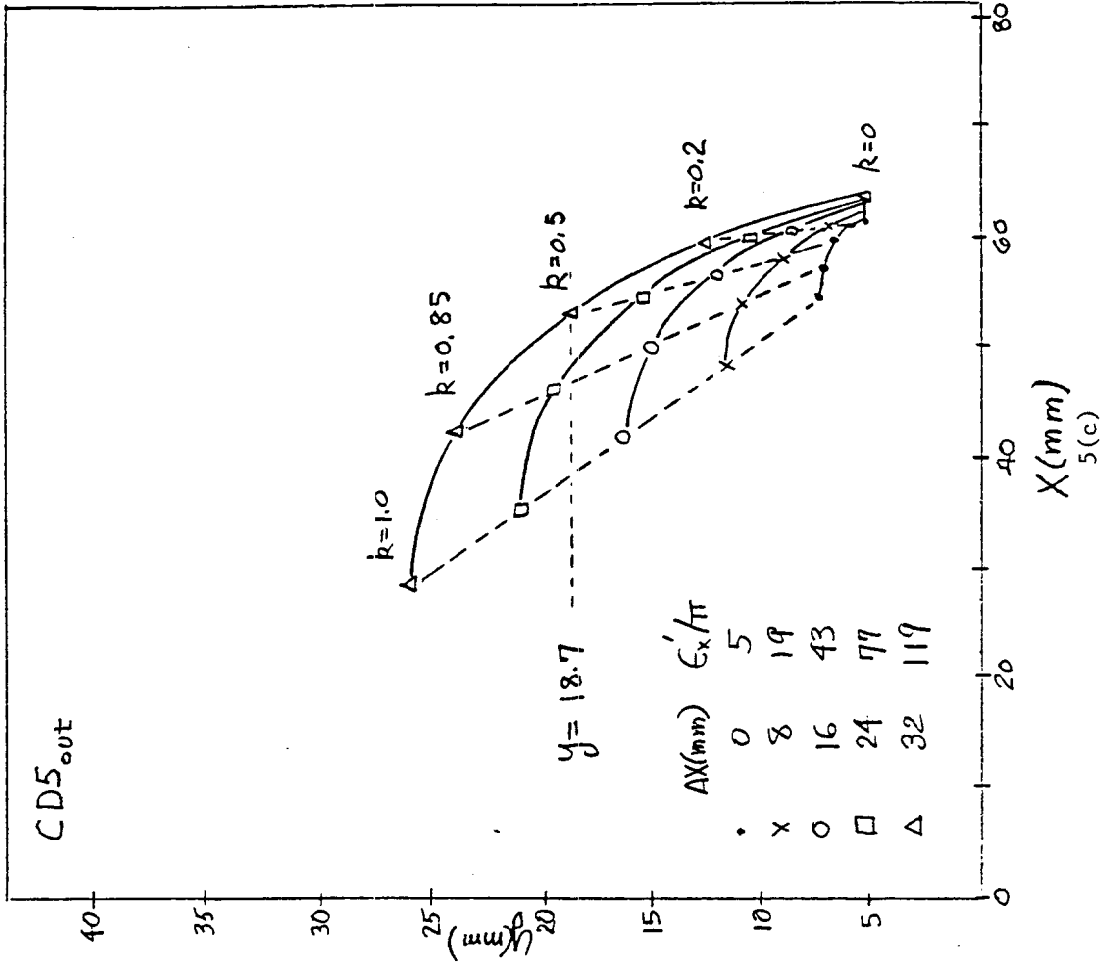
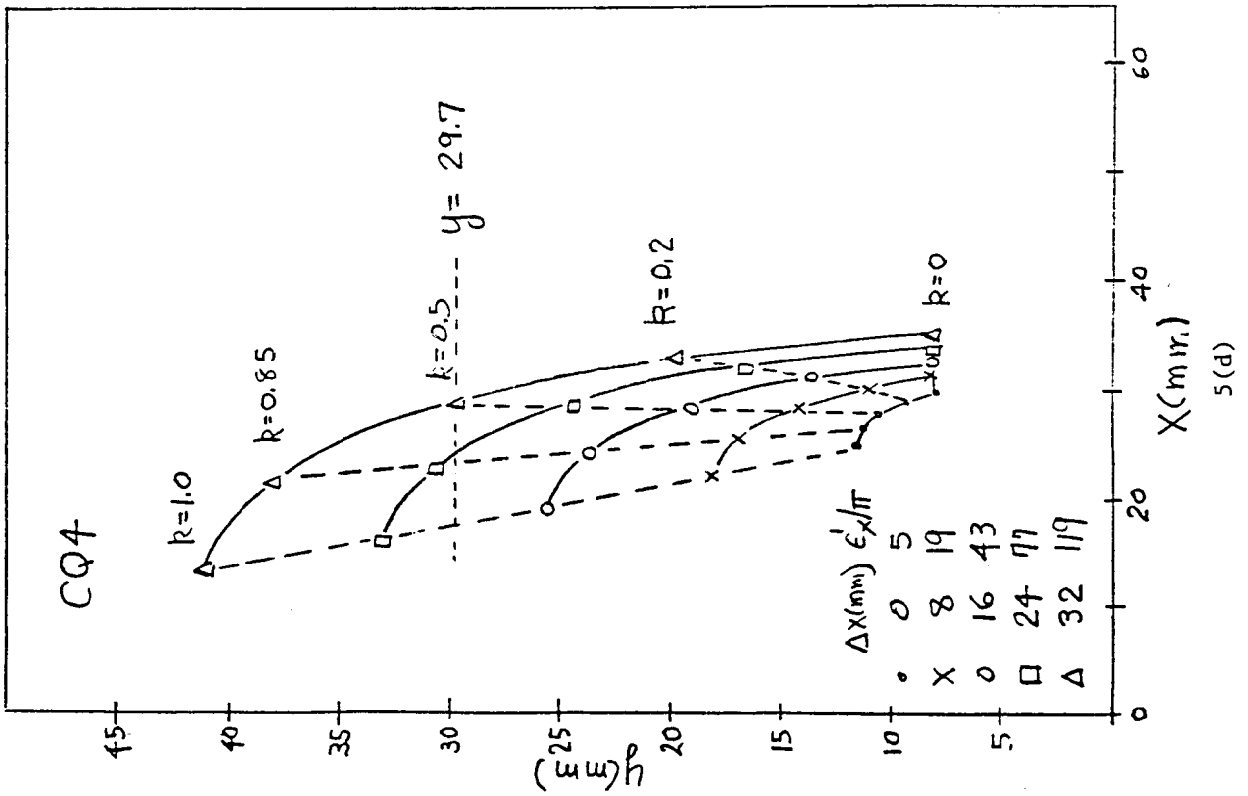
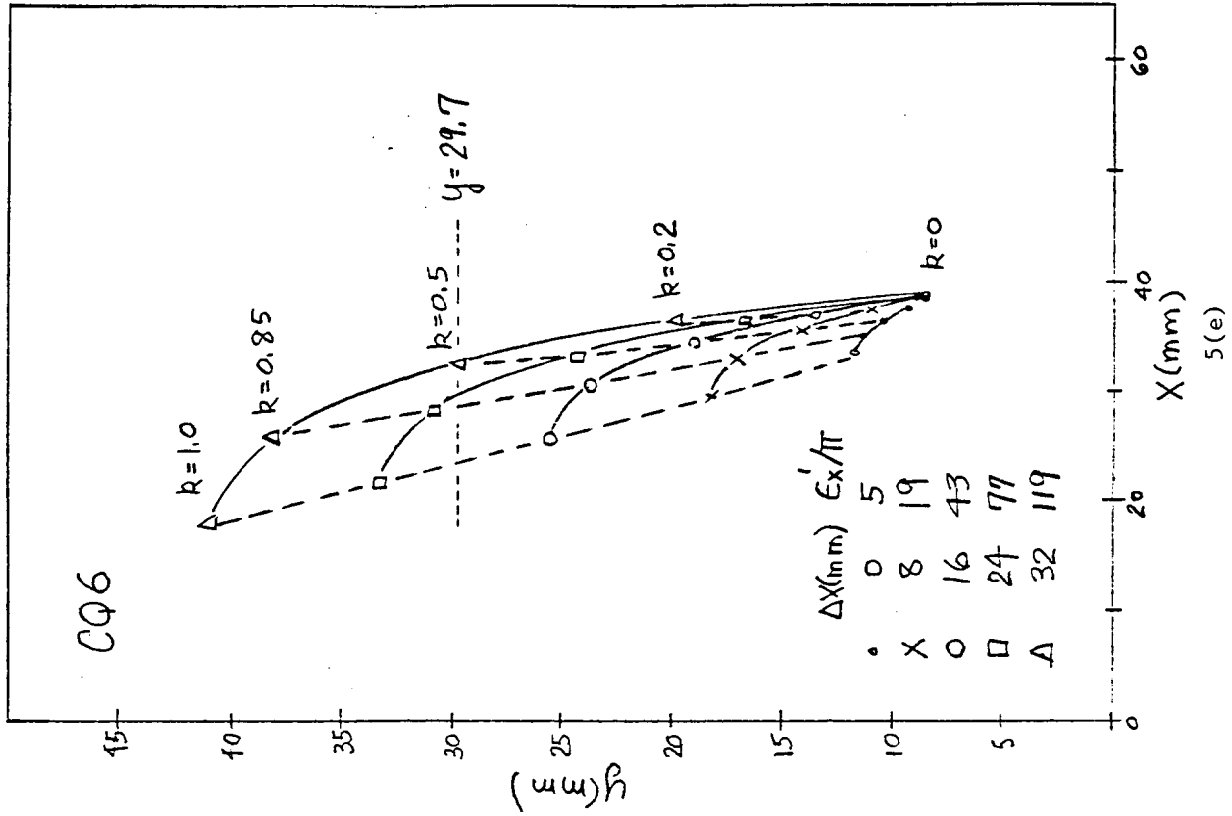


Figure 5(a). Maximum x and y needed at quadrupole CQ5 for several combinations of ΔX , the distance of the closed orbit from the center of the injection channel, and k , the portion of the horizontal emittance transferred to the y motion. The dashed line at $y = 15.5$ mm corresponds to the maximum amplitude that will fit into the elliptical chamber at 40 mm from its centerline ($A_y = 28.5$ mm) when the particle is near defocusing quadrupoles.



Figures 5(b) and 5(c). Maximum x and y needed at the upstream end (5(b)) and downstream end (5(c)), respectively, of dipole CD5 for various combinations of ΔX and k , the portion of the horizontal emittance transferred to the vertical motion. The dashed lines at $y = 27.9$ mm (b) and $y = 18.7$ mm (c) correspond to the maximum vertical amplitude that fits into the elliptical chamber at 40 mm from its centerline when the particle is near defocusing quadrupoles.



Figures 5(d) and 5(e). Maximum x and y needed at the centers of quadrupoles CQ4 and CQ6 for several combinations of ΔX , the distance of the closed orbit from the center of the injection channel, and k , the portion of the horizontal emittance transferred to the vertical motion. Dashed lines at $y = 29.7$ mm correspond to the maximum vertical amplitude that fits into the elliptical chamber at 40 mm from its centerline when the particle is near defocusing quadrupoles.

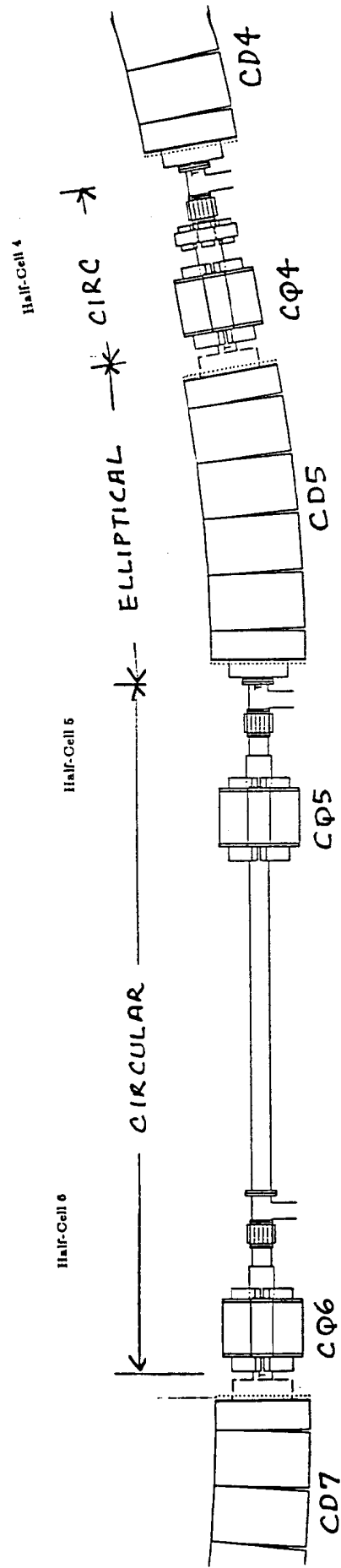


Figure 6. Area of period "C" where the orbit bump is maximum. Only dipoles CD5 and CD7 have elliptical chambers; all quadrupoles have circular chambers of 6" diameter. The symbols "T" on the chamber center-line near dipole ends indicate transitions from an elliptical to a circular chamber. The aperture will be limited at the transitions nearest to defocusing (even numbered) quadrupoles.